Clinical Radiology xxx (xxxx) xxx

Contents lists available at ScienceDirect

Clinical Radiology

journal homepage: www.clinicalradiologyonline.net

A radiomics–clinical nomogram for preoperative prediction of IDH1 mutation in primary glioblastoma multiforme

X. Su [a,f,1], H. Sun [a,1], N. Chen [b], N. Roberts [c], X. Yang [d], W. Wang [a], J. Li [e], X. Huang [a], Q. Gong [a,**], Q. Yue [d,f,*]

[a] *Huaxi MRI Research Center (HMRRC), Department of Radiology, West China Hospital of Sichuan University, Chengdu, China*
[b] *Department of Pathology, West China Hospital of Sichuan University, Chengdu, China*
[c] *Edinburgh Imaging, School of Clinical Sciences, The Queens Medical Research Institute (QMRI), University of Edinburgh, Edinburgh, United Kingdom*
[d] *Department of Radiology, West China Hospital of Sichuan University, Chengdu, China*
[e] *The Center of Gerontology and Geriatrics, West China Hospital, Sichuan Universtiy, Chengdu, Sichuan, 610041, China*
[f] *Huaxi Glioma Center, West China Hospital of Sichuan University, Chengdu, China*

ARTICLE INFORMATION

Article history:
Received 17 March 2020
Accepted 31 July 2020

AIM: To develop and validate an individualised radiomics–clinical nomogram for the prediction of the isocitrate dehydrogenase 1 (IDH1) mutation status in primary glioblastoma multiforme (GBM) based on radiomics features and clinical variables.

MATERIALS AND METHODS: In a retrospective study, preoperative magnetic resonance imaging (MRI) images were obtained of 122 patients with primary glioblastoma (development cohort = 101; validation cohort = 21). Radiomics features were extracted from total tumour based on the post-contrast high-resolution three-dimensional (3D) T1-weighted MRI images. Radiomics features were selected by using a least absolute shrinkage and selection operator (LASSO) binomial regression model with nested cross-validation. Then, a radiomics–clinical nomogram was constructed by combining relevant radiomics features and clinical variables and subsequently tested by using the independent validation cohort.

RESULTS: A total of 105 features were quantified on the 3D MRI images of each patient, and eight were selected to construct the radiomics model for predicting IDH1 mutation status. The mean classification accuracy and mean κ value achieved with the model were 88.4±3% and 0.701±0.08, respectively. The radiomics–clinical nomogram, which combines eight radiomics features and three clinical variables (patient age, sex and tumour location), demonstrated good discrimination (C-index 0.934 [95% CI, 0.874 to 0.994]; F1 score 0.78) and performed well with the validation cohort (C-index 0.963 [95% CI, 0.957 to 0.969]; F1 score 0.91; AUC 0.956).

* Guarantor and correspondent: Q. Yue, Department of Radiology, West China Hospital of Sichuan University, #37 GuoXue Xiang, Chengdu Sichuan, 610041, China. Tel.: +86(0)2885421065; fax: +86(0)2885422746.
** Guarantor and correspondent: Q. Gong, Huaxi MRI Research Center (HMRRC), Department of Radiology, West China Hospital of Sichuan University, Chengdu, 610041, China. Tel./fax: +86(0)2885423503.
E-mail addresses: qiyonggong@hmrrc.org.cn (Q. Gong), scu_yq@163.com (Q. Yue).
[1] These authors contributed equally to this work.

https://doi.org/10.1016/j.crad.2020.07.036

Please cite this article as: Su X et al., A radiomics–clinical nomogram for preoperative prediction of IDH1 mutation in primary glioblastoma multiforme, Clinical Radiology, https://doi.org/10.1016/j.crad.2020.07.036

CONCLUSIONS: A radiomics–clinical nomogram was developed and proved to be valuable in the non-invasive, individualised prediction of the IDH1 mutation status in patients with primary GBM. The nomogram can be applied using clinical conditions to facilitate preoperative patient evaluation.

Introduction

Glioblastoma multiforme (GBM) is the most common malignant tumour of the central nervous system (CNS), and its prognosis is usually poor.[1] Glioblastomas are mainly divided into isocitrate dehydrogenase (IDH)-wildtype and IDH-mutated GBM depending on the IDH mutation status.[2] The identification of IDH mutations in GBM has provided a better understanding of tumour biology.[3] Patients with IDH1/2-mutant GBM were reported to have a longer overall survival than those with IDH-wildtype GBM (31 versus 15 months).[4] The IDH1 mutation is more common than the IDH2 mutation and may become a key target for therapies. Early determination of IDH1 mutation status may help the development of optimal treatment strategies,[5] and a non-invasive approach would be of great value.

It has been shown that radiographic features extracted from magnetic resonance imaging (MRI) images are associated with gene expression signatures and histological subtypes.[6] In patients with IDH1-wildtype glioma, peripheral enhancement was related to poor progression-free survival and poor overall survival[7]; however, qualitative assessment of image features can be highly dependent upon observer experience, limiting the precision, and reproducibility of the results.[8].

Most recently, radiomics approaches have been widely used to predict molecular markers such as IDH1 and TP53, as well as 1p/19q codeletion status in gliomas.[9–11] According to these studies, radiomics has the potential to estimate the IDH1 mutation status and improve decision-making in the management of GBM. Previous radiomics studies of GBM and the IDH1 mutation have, however, investigated gliomas of mixed grades and have mostly used only radiomics features despite the possible usefulness of clinical variables such as tumour location and patient age.[12,13]

The aim of the present study was to predict IDH1 mutation status non-invasively in newly diagnosed primary GBM. It was hypothesised that a radiomics–clinical nomogram that incorporated both radiomics features and clinical information would be effective for this purpose and might perform better than a radiomics- or clinical feature-only model. Three-dimensional (3D) T1-weighted MRI was used to develop and validate the prediction model, as previous studies have shown that thin-section images can improve the reproducibility of extracted features and thus make the model more effective.[14–16]

Materials and methods

Patient enrolment

The institutional review board approved this retrospective study and waived the requirement to obtain informed consent. The study population, comprising patients with brain tumours who underwent MRI at West China Hospital of Sichuan University, was recruited by X. Su, with 3 years of diagnostic experience, between January 2011 and December 2017, and an independent validation cohort was recruited by W. Wang, with 3 years of experience, between January 2018 and November 2019. The following inclusion criteria were applied: (1) histopathologically confirmed primary glioblastoma according to the current World Health Organization (WHO) classification of tumours of the CNS[2], (2) confirmed IDH1 mutation status, (3) available preoperative MRI images obtained using identical protocols and comprising pre- and post-contrast T1-weighted magnetisation-prepared rapid acquisition gradient echo (MPRAGE) images, fluid attenuated inversion recovery (FLAIR) images and axial T2-weighted images. A total of 122 newly diagnosed GBM patients met these criteria and served as the patient population investigated in the present study (divided into a development cohort of 101 patients and a validation cohort of 21 patients). Sixteen patients were excluded due to (1) a lack of preoperative T1-MPRAGE images ($n = 11$); (2) no contrast enhancement of the tumours ($n = 3$); or (3) motion artefacts on MRI images ($n = 2$). The Mann–Whitney *U*-test, chi-squared test, and Fisher's exact test were employed to assess differences in clinical variables, and the statistical significance level was set at 0.05.

MRI acquisition and image post-processing

Images for all patients were obtained in the course of routine clinical work-up using a Skyra or Trio Tim 3 T or Avanto 1.5 T MRI system (Siemens Healthier, Erlangen, Germany) using either an 8-channel head matrix or a 20-channel coil. The MRI protocol comprises non-enhanced sagittal and axial T1-weighted, axial T2-weighted and T2-weighted FLAIR images and post-contrast sagittal 3D T1-weighted MPRAGE images. The main acquisition parameters for the 3D T1-weighted images were TR=1,600 ms/TE=2.3 ms, 176 sections, section thickness = 1 mm, matrix size = 256×232 and field of view (FOV) = 217×240 mm. Identification of the extent of the whole tumour (which

Please cite this article as: Su X et al., A radiomics–clinical nomogram for preoperative prediction of IDH1 mutation in primary glioblastoma multiforme, Clinical Radiology, https://doi.org/10.1016/j.crad.2020.07.036

typically comprised regions of contrast enhancement, non-contrast enhancement, and necrosis) was mainly based on inspection of the T1-weighted 3D MPRAGE images.

Region of interest (ROI) delineation

The 3D T1-weighted MPRAGE images of all the patients were skull stripped using the FSL library to isolate the brain[17]. Subsequently, ITK-SNAP Software (version 3.6.0, http://www.itksnap.org) was used to perform semi-automatic segmentation of the tumour using the active contour method. Semi-automatic segmentation reduces inter-operator variability as well as the time to segment ROIs. The ROI boundary typically included regions of contrast enhancement, non-contrast enhancement, and necrosis/cysts.[18] The results of the segmentation were always checked visually and edited as appropriate by an experienced neuroradiologist (Electronic Supplementary Material Fig. S1). Both the operator (X. Su) and the supervisor (Q. Yue) were blinded to the IDH mutation status as well as the clinical information.

MRI feature extraction, selection, and nested cross-validation

For each of the segmented ROI volumes in the 3D T1-weighted image, seven different categories of features were extracted using PyRadiomics software (http://pyradiomics.readthedocs.io) first-order features, shape-features, grey level co-occurrence matrix (GLCM) features, grey level run length matrix (GLRLM) features, grey level size zone matrix (GLSZM) features, neighbouring grey tone difference matrix (NGTDM) features, and grey level dependence matrix (GLDM) features.[19] Detailed descriptions were provided in a previous publication.[20] In the present study, the major settings for feature extraction were as follows: “resampledPixelSpacing” = (1, 1, 1), “normalise” = true, and “normaliseScale” = 100.

First, 10 classifier models were generated to select the most valuable image features according to the mean importance rank. Repeated nested cross-validation (10-fold), available in the “*caret*” package (i.e., classification and regression training) written for R software (Version 3.6, http://www.r-project.org), was used to avoid overfitting and to select image features.[21] The performance of the classifier was measured by overall accuracy, sensitivity, specificity and the κ score. Then, a logistic regression model was built based on the selected features using the least absolute shrinkage and selection operator (LASSO) binomial regression model available in the“*glmnet*” package (i.e., elastic net model paths for some generalised linear models) written using R software, which is suitable for the regression of high-dimensional data with a relatively small sample size.[22] Furthermore, as described in a previous study, a radiomics score (RAD-score) was computed for each GBM patient as a linear combination of selected features weighted by their respective coefficients.[23]

Radiomics and radiomics–clinical nomogram construction

The radiomics–clinical nomogram developed in this study, combining radiomics features and clinical variables (age, sex, and tumour location), was constructed using the package “*rms*”, written in R software. The clinical information was included to enhance the radiomics nomogram. A study of prognostic prediction demonstrated that radiomics nomograms can perform better than clinical nomograms[23]. The performances of the clinical nomogram, radiomics model, and radiomics–clinical nomogram were also compared in the present study. Harrell’s significant concordance index (C-index) was used to quantify the discriminability of the radiomics–clinical nomogram using the package “*Hmisc*”, written in R software. In the present study, the C-index was computed using 1,000 bootstrap resamples. A C-index of 1 indicates perfect concordance, and a C-index of 0.5 indicates concordance no better than chance.[24] An overview of the workflow is shown in Fig 1. In addition, to better evaluate the classification ability of the present model, the F1 score was also calculated to evaluate the radiomics–clinical model performance based on a balance between precision and recall.[25]

Validation of the radiomics and radiomics–clinical nomogram

Validation of the model was performed using R software. In particular, the predictive performance of the selected features was assessed for the validation cohort by calculating the accuracy, sensitivity, specificity, area under curve (AUC) and F1 score using the *caret, pROC and InformationValue* packages in R software. Then, the performance of the radiomics–clinical nomogram was tested for the validation cohort with the logistic regression formula formed for the development cohort. Finally, the total score for each patient and the overall C-index were calculated.

RESULTS

Clinical characteristics

Detailed demographic characteristics of the patients are presented in Table 1. The development cohort comprised 101 GBM patients, including 74 patients (5–80 years) with IDH1-wildtype GBM and 27 patients (16–79 years) with IDH1 mutated GBM (see Electronic Supplementary Material Fig. S2). The independent validation cohort included 21 patients (11–72 years), 15 IDH1-wildtype GBM and six patients (22–37 years) with IDH1 mutated GBM. Although the mean age of patients with the IDH1 mutation was lower than that of patients with IDH1-wildtype GBM in the development cohort (mean age, 50.24 versus 42.29 years, $p = 0.012$), this difference was not significant in the validation cohort (mean age, 44.6 versus 38.5 years, $p = 0.36$).

Please cite this article as: Su X et al., A radiomics–clinical nomogram for preoperative prediction of IDH1 mutation in primary glioblastoma multiforme, Clinical Radiology, https://doi.org/10.1016/j.crad.2020.07.036

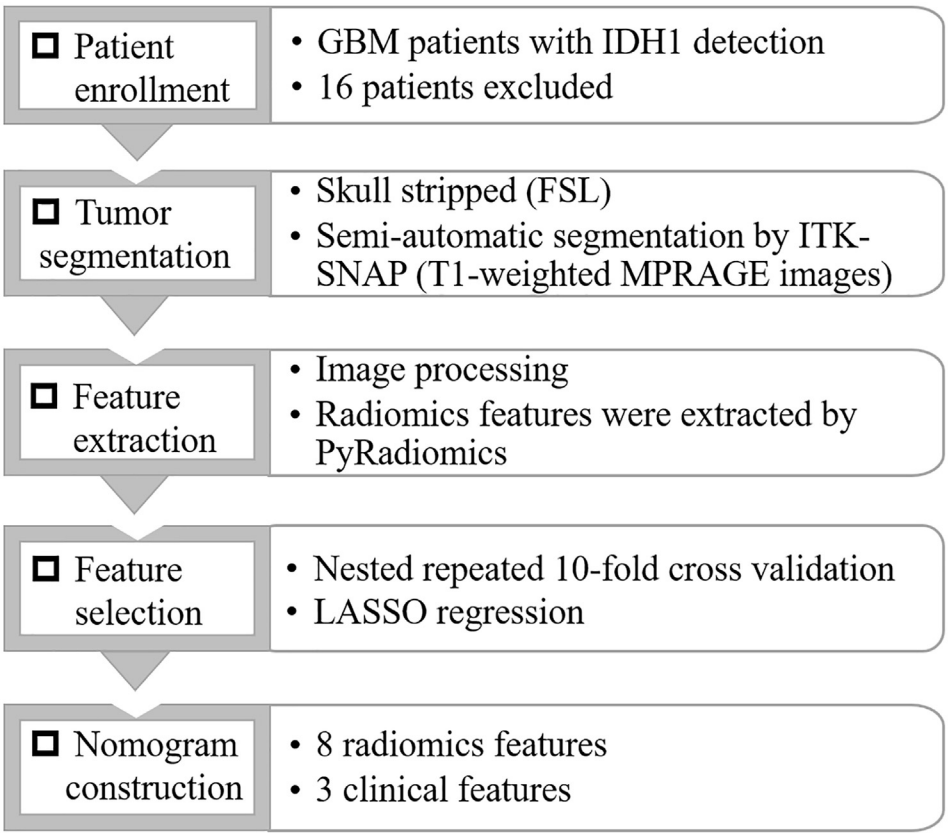

Figure 1 Workflow of the construction of the radiomics nomogram in the current study.

Most IDH1-mutated tumours occurred in males and were located in the right hemisphere, although no significant difference in sex was found between the two groups in either the development or the validation cohort ($p > 0.05$, see details in Table 1).

Radiomics features and classification performance

For each patient, a total of 105 radiomic features were extracted from the ROI, including 18 first-order features, 14 shape features, 22 GLCM features, 16 GLRLM features, 16 GLSZM features, 5 NGTDM features, and 14 GLDM features. By applying the nested cross-validation procedure, these initial 105 features were ranked by their importance scores for the radiomics prediction model. First, the 20 most important image features were selected from 10 classification models according to the importance rank. Then, the eight most relevant predictors of these features were selected by the λ value in the LASSO model for construction of the classifier: the first order feature

Table 1
Clinical characteristics of glioblastoma multiforme patients.

	Development cohort ($n = 101$)			Validation cohort ($n = 21$)		
	IDH1 wild-type ($n = 74$)	IDH1 mutation ($n = 27$)	p-Value	IDH1 wild-type ($n = 15$)	IDH1 mutation ($n = 6$)	p-Value
Age (years)	50.24±18.61	42.29±17.44	0.012[ac]	44.6±10.52	38.5±18.58	0.36[c]
<18 years	7.71±2.14	16		11	NA	
>18–65 years	54.68±13.07	43.31±16.95		47±16.52	38.5	
Gender			0.378[b]			0.336[b]
Male	50	15		8	5	
Female	24	12		7	1	
Tumour location in brain			0.014[d]			0.203[d]
Left	26	8		8	1	
Right	36	18		6	5	
Bilateral	12	1		1	0	

IDH, isocitrate dehydrogenase.
[a] $p<0.05$.
[b] Chi-square test.
[c] Mann–Whitney *U*-test.
[d] Fisher's exact test.

Please cite this article as: Su X et al., A radiomics–clinical nomogram for preoperative prediction of IDH1 mutation in primary glioblastoma multiforme, Clinical Radiology, https://doi.org/10.1016/j.crad.2020.07.036

skewness, shape features sphericity and elongation, GLCM features correlation, cluster shade and inverse difference, the GLDM feature large dependence high grey level emphasis (LDHGLE) and the GLRLM feature grey level non-uniformity (GLN; Electronic Supplementary Material Table S1, Fig 2). The LASSO coefficient profile showed that the optimal lambda results could be obtained using just eight non-zero coefficients (Electronic Supplementary Material Fig. S3). The classification accuracy and κ value of the 10 classification models created using repeated 10-fold cross-validation were 88.4±3% and 0.701±0.08, respectively. The sensitivity and specificity for the classification were 94.6±6.9% and 73.3±13%, respectively.

The RAD score based on the eight radiomics features selected through the LASSO model was calculated using the following formula:

RAD-score=−3.519446−2.800307×Elongation−4.638266×Sphericity+0.1304058× Skewness+0.0000121777×ClusterShade+3.043114×Correlation+1.645184×Id+ 0.000219206×GLN+0.00002877556×LDHGLE

Radiomics–clinical nomogram

The AUC of the clinical nomogram model constructed with age, sex, and tumour location was 0.76, and the AUC of the single RAD-score nomogram model was 0.894; however, the radiomics–clinical nomogram, combining the RAD-score and the clinical variables, had a higher AUC of 0.934. The radiomics–clinical nomogram of the validation cohort is presented in Fig 3 and represents an individualised prediction model for the IDH1 mutation status. The total score for each patient was obtained by adding the scores of age, sex, tumour location, and RAD-score, with the latter two having greater weights (Fig 3). The C-index of the radiomics–clinical nomogram was 0.934 (95% CI, 0.874 to 0.994), which is higher than that of the nomogram based only on the clinical variables (C-index 0.76) or only on the RAD-score (C-index 0.894). The corrected C-index for the development cohort was 0.909 via 1,000 bootstrap resamples. The corrected C-index of the radiomics–clinical nomogram when used to predict the IDH1 mutation status in the validation cohort was 0.963 (95% CI, 0.957 to 0.969) (see Electronic Supplementary Material Fig. S4–S5). The radiomics–clinical nomogram performed better than the radiomics-only model with the development cohort (nomogram C-index 0.931; radiomics-only model C-index 0.858), though not with the validation cohort (C-index 0.879 and 0.96 for the nomogram and radiomics-only model, respectively). Furthermore, the F1 score of the radiomics–clinical nomogram was 0.78 with the development cohort and 0.91 with the validation cohort (Fig 4).

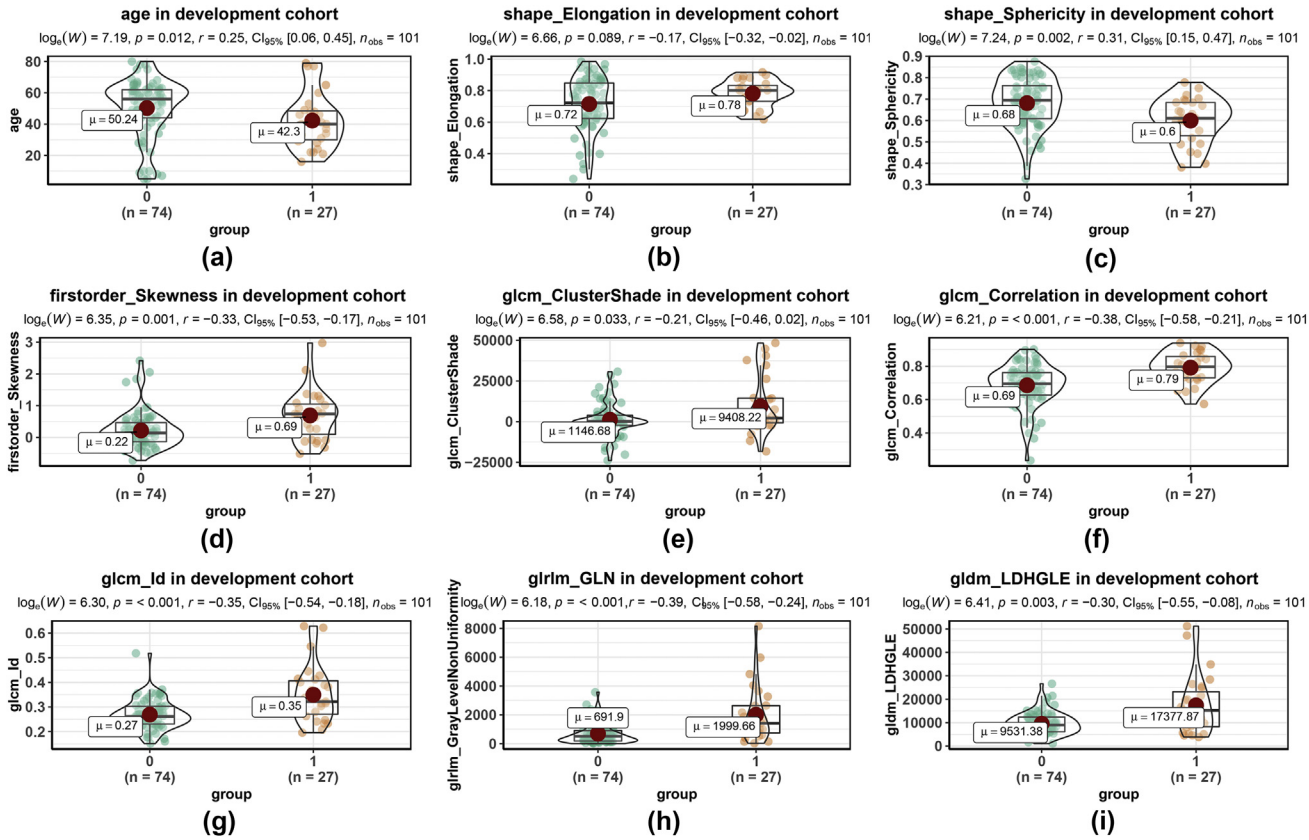

Figure 2 The eight features that best discriminate IDH1-mutant from IDH1-wildtype glioblastoma patients, i.e., age, the shape features elongation and sphericity, the GLCM features cluster shade, correlation and Id, the GLRLM feature grey level nonuniformity and the GLDM feature LDHGLE.

Please cite this article as: Su X et al., A radiomics–clinical nomogram for preoperative prediction of IDH1 mutation in primary glioblastoma multiforme, Clinical Radiology, https://doi.org/10.1016/j.crad.2020.07.036

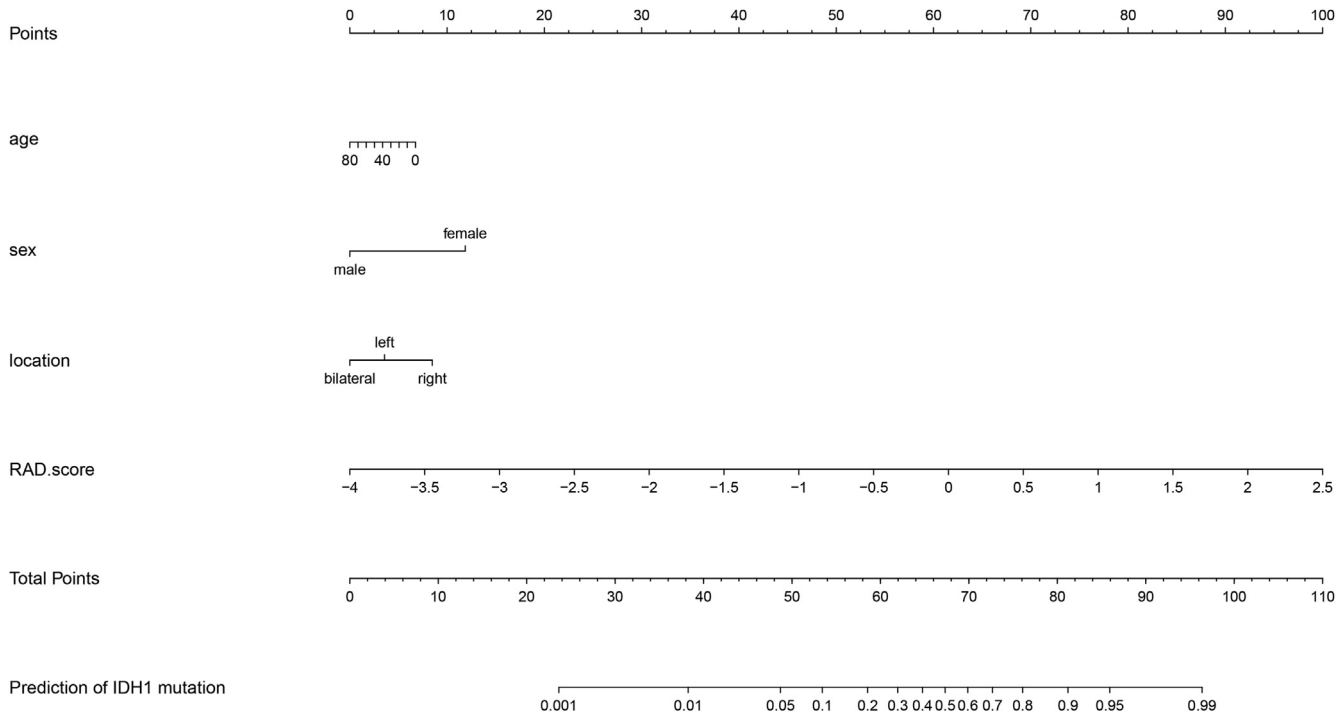

Figure 3 Nomogram constructed from the radiomics features and clinical variables extracted from the development cohort, including age, sex, tumour location, and RAD-score. The total points are calculated.

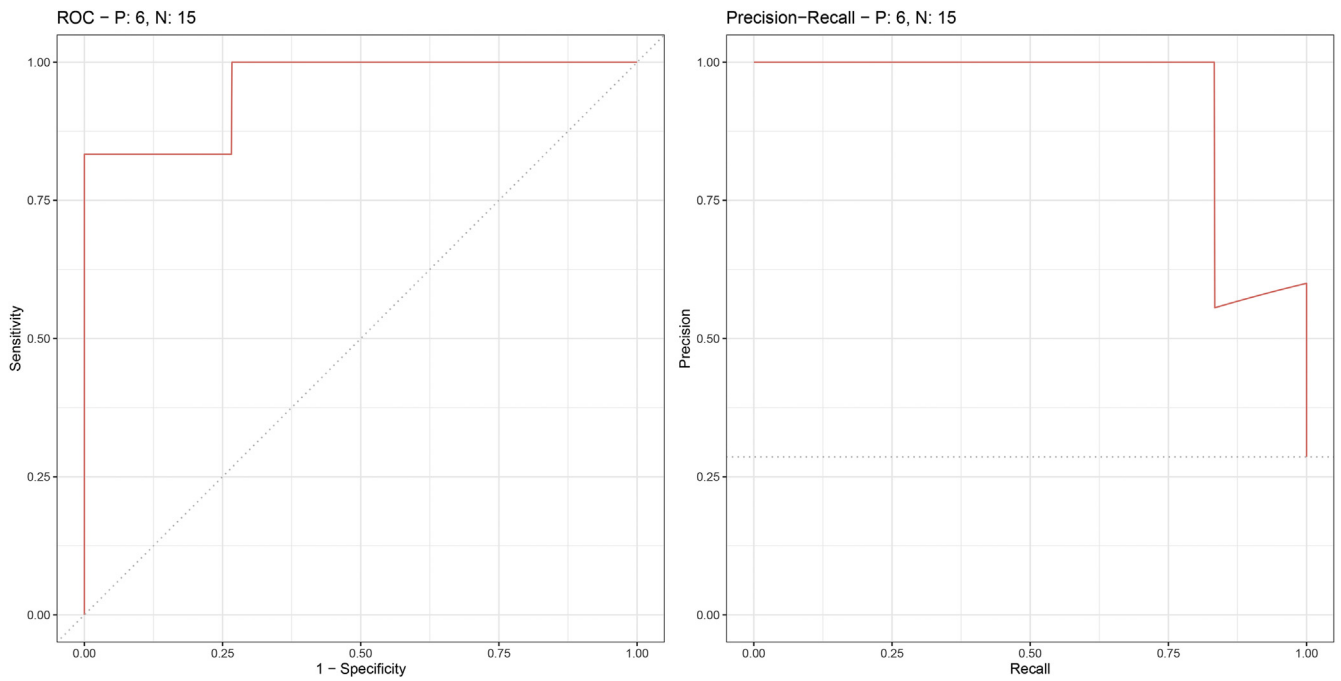

Figure 4 The ROC curve and precision-recall curve of the validation cohort.

Please cite this article as: Su X et al., A radiomics–clinical nomogram for preoperative prediction of IDH1 mutation in primary glioblastoma multiforme, Clinical Radiology, https://doi.org/10.1016/j.crad.2020.07.036

Discussion

The main contribution to the radiomics–clinical nomogram was the analysis of 3D T1-weighted MRI images obtained with contrast enhancement for 110 patients with newly diagnosed GBM. For each ROI, 105 quantitative image features were extracted. The final model contained eight imaging features, and a nomogram was created using these features together with clinical data to predict IDH1 mutation status, which showed excellent performance (C-index = 0.963).

The benefit to patient management at the early stage of the disease and in follow-up of the non-invasive prediction of the IDH mutation status of glioma using MRI has been demonstrated in several previous studies.[9,10,14] A recent study reported the prediction of the IDH1 mutation status in GBM based on 31 features from preoperative multiparametric MRI images,[12] but they did not take radiomics features into consideration nor did they incorporate clinical features into the model. Another radiomics study on the IDH1 mutation in low-grade glioma also showed that a stratifying strategy helped to predict the IDH1 mutation status; unfortunately, however, the relatively small patient population (only 57 patients) and the absence of a validation cohort reduced its power.[13] In the present study, the LASSO algorithm with nested cross-validation, which has been used in other radiomics research,[23] was used to overcome the over-sampling problem and efficiently reduce the dimensionality of the radiomics features. During the construction of the classification models, the average classification accuracy and κ value achieved with repeated 10-fold cross-validation were 88.4±3% and 0.701±0.08, respectively, which reflected the effectiveness of the feature selection procedure. Furthermore, as the radiomics features extracted from MRI images depend on the image resolution,[26] analysis of 3D high-resolution MRI images is preferable.[16] For this reason, the radiomics features used in the present study were extracted from images with an isotropic resolution of 1 mm that were acquired using the same MRI system. Robust tumour segmentation was also a critical step in the workflow to produce the radiomics–clinical model. The semi-automatic segmentation algorithm saves time and has been shown to have higher reproducibility than manual segmentation[27] and to even be helpful for the planning of gamma knife treatments of brain lesions.[28] Although the automatic segmentation method was explored in the Brain Tumour Segmentation Challenge (BRATS), the performance of the model was not always robust for different BRATS databases.[29] Further enhancements in image contrast will potentially increase reproducibility and expand clinical usefulness.[30] Previously, it had been reported that IDH mutations are likely to be related to less contrast enhancement on MRI.[31] The model obtained from contrast imaging could add helpful information for predicting IDH1 mutation status. Thus, the methodology of this study is robust in terms of feature selection. Based on the use of advanced analysis techniques and strict quality-assurance procedures, individualised prediction of the IDH1 mutation status was achieved in GBM patients.

Among the selected radiomics features, the first-order features describe the distribution of voxel intensities within the region of interest, and skewness reflects the asymmetry of the distribution of these values.[32] In particular, the tail was extended towards the positive directions in the IDH1-wildtype GBM group, which indicated that the mean grey level skewed to a higher value (Fig 2). Shape features describe the three-dimensional size and shape of the ROI,[19] in which sphericity is a measure of how close the shape of the tumour is to a sphere and elongation is associated with the length of the tumour diameter. From these shape features, it can be seen that IDH1-mutant tumours have a greater shape elongation than IDH1-wildtype tumours (Fig 2b), which indicates that they are less spherical. The GLCM feature of correlation shows the linear dependency of the grey-level values on their respective voxels. A higher value of correlation and inverse difference (Id) is associated with homogeneity,[33] which in this study likely means less variability in the IDH1-mutant group. Moreover, cluster shade is sensitive to tumour heterogeneity, which could help predict distant metastasis in lung adenocarcinoma.[34] A higher value in the IDH1-mutant group implies greater asymmetry about the tumour. The GLN feature of GLRLM is a measure of the similarity of grey-level intensity values in the MRI image, and the higher value in the IDH1-mutant group indicates a lower similarity in intensity values (Fig 2). A previous study of gastrointestinal stromal tumours showed that normalised GLN values were linked to tumour mutations.[35] Finally, the GLDM feature referred to as LDHGLE is a measure of the joint distribution of large dependences with higher grey-level values, and a greater value means that higher grey-level voxels were adjacent to each other[19] and less inhomogeneous to the tumour.[36] In summary, the radiomics features relating to shape, heterogeneity, and signal intensity contributed most to the predictive model; in previous radiomics studies, these same features were applied to predict the IDH genotype in diffuse gliomas with high accuracy.[10] The present study gives the impression that compared with those of IDH1-wildtype GBM, IDH1-mutant GBM tumours are less spherical (due to greater shape elongation) but more homogeneous (due to less necrosis/fewer cystic changes or haemorrhage) with lower mean signal intensity (due to less contrast enhancement).[37]

The final radiomics–clinical nomogram produced in the present study was derived from eight radiomics features and three clinical variables, namely, age, sex, and tumour location. A previous clinical study showed that the age distribution, male/female ratio and tumour location were different in patients with IDH1-wildtype and IDH1 mutation status.[4] The present radiomics–clinical nomogram showed excellent performance in predicting the IDH1 mutation status (C-index = 0.934), outperforming the model based only on radiomics features (C-index = 0.894) or only on clinical features (C-index=0.76) with the development cohort. In addition, the high F1 score obtained with the

Please cite this article as: Su X et al., A radiomics–clinical nomogram for preoperative prediction of IDH1 mutation in primary glioblastoma multiforme, Clinical Radiology, https://doi.org/10.1016/j.crad.2020.07.036

validation cohort indicated good performance of the radiomics–clinical nomogram. Nomograms have been widely used for risk stratification and prediction of other diseases[23,38–41] and have been found to outperform expert clinicians in predicting outcome.[39,42] A nomogram is a visual representation of a statistical model and allows for different weightings of various factors.[38] With regard to the clinical variables included in the radiomics–clinical nomogram in the present study, sex had slightly more influence than age and tumour location. The proportion of male patients was larger than that of female patients in the IDH1-mutant group in the present study. This finding is consistent with a previous study in which the male/female ratio was higher among primary GBM patients with the IDH1 mutation than among those without the IDH1 mutation (though $p > 0.05$).[43] In addition, the absence of the IDH mutation has also been reported to be related to tumour location in low-grade gliomas (LGGs).[44] In the present study, IDH1-mutated GBM was found to be preferentially located in the right hemisphere. Regarding age, Parsons *et al.* (2008) previously reported that IDH1 mutations occurred in a large fraction of young patients with GBM,[3] which is consistent with the present study. The fact that age and location have low weight in predicting IDH1 mutations may be related to the relatively small sample size.

The present study has several limitations. First, a relatively small number of IDH1-mutated GBM patients were included in the study. This is due to the low frequency of the IDH1 mutation in primary glioblastomas (8.8%)[43] as well as the strict eligibility requirements for both MRI parameters and genetic data. Although nested cross-validation provides an almost unbiased estimate of the true error, a future study with a larger cohort is still needed to further improve the performance of the algorithm. Furthermore, although the present study revealed the highly predictive value of contrast-enhanced MRI images, other imaging methods could also be incorporated to enhance the prediction power for IDH1 mutation status.

In conclusion, a radiomics–clinical model based on clinical variables and radiomics features derived from post-contrast high-resolution 3D T1-weighted MRI images was constructed. The nomogram can predict the IDH1 mutation status non-invasively in newly diagnosed primary GBM, and it outperformed a model based only on radiomics features or clinical information. This kind of model can benefit clinical practice from the start of disease management.

Conflict of interest

The authors declare no conflict of interest.

Acknowledgements

This work was supported by the Sichuan Provincial Foundation of Science and Technology (grant nos. 2019YFS0428, 2018SZ0175) and the Foundation of the National Clinical Research Center for Geriatrics (grant no. Z2018A07).

Appendix A. Supplementary data

Supplementary data to this article can be found online at https://doi.org/10.1016/j.crad.2020.07.036.

References

1. Ostrom QT, Gittleman H, Fulop J, *et al.* CBTRUS statistical report: primary brain and central nervous system tumors diagnosed in the United States in 2008–2012. *Neuro Oncol* 2015;**17**(Suppl. 4):iv1–62.
2. Louis DN, Perry A, Reifenberger G, *et al.* The 2016 World Health Organization classification of tumors of the central nervous system: a summary. *Acta Neuropathol* 2016;**131**(6):803–20.
3. Parsons DW, Jones S, Zhang X, *et al.* An integrated genomic analysis of human glioblastoma multiforme. *Science* 2008;**321**(5897):1807–12.
4. Ohgaki H, Kleihues P. The definition of primary and secondary glioblastoma. *Clin Canc Res* 2013;**19**(4):764–72.
5. Turkalp Z, Karamchandani J, Das S. IDH mutation in glioma: new insights and promises for the future. *JAMA Neurol* 2014;**71**(10):1319–25.
6. Ellingson BM. Radiogenomics and imaging phenotypes in glioblastoma: novel observations and correlation with molecular characteristics. *Curr Neurol Neurosci Rep* 2015;**15**(1):506.
7. Wang K, Wang Y, Fan X, *et al.* Radiological features combined with IDH1 status for predicting the survival outcome of glioblastoma patients. *Neuro Oncol* 2016;**18**(4):589–97.
8. Han Y, Xie Z, Zang Y, *et al.* Non-invasive genotype prediction of chromosome 1p/19q co-deletion by development and validation of an MRI-based radiomics signature in lower-grade gliomas. *J Neurooncol* 2018;**140**(2):297–306.
9. Yu J, Shi Z, Lian Y, *et al.* Noninvasive IDH1 mutation estimation based on a quantitative radiomics approach for grade II glioma. *Eur Radiol* 2017;**27**(8):3509–22.
10. Zhang B, Chang K, Ramkissoon S, *et al.* Multimodal MRI features predict isocitrate dehydrogenase genotype in high-grade gliomas. *Neuro Oncol* 2017;**19**(1):109–17.
11. Wu S, Meng J, Yu Q, *et al.* Radiomics-based machine learning methods for isocitrate dehydrogenase genotype prediction of diffuse gliomas. *J Canc Res Clin* 2019;**145**(3):543–50.
12. Lee MH, Kim J, Kim ST, *et al.* Prediction of IDH1 mutation status in glioblastoma using machine learning technique based on quantitative radiomic data. *World Neurosurg* 2019;**125**:e688–96.
13. Ren Y, Zhang X, Rui W, *et al.* Noninvasive prediction of IDH1 mutation and ATRX expression loss in low-grade gliomas using multiparametric MRI radiomic features. *J Magn Reson Imag* 2019;**49**(3):808–17.
14. Chang K, Bai HX, Zhou H, *et al.* Residual convolutional neural network for the determination of IDH status in low- and high-grade gliomas from MR imaging. *Clin Canc Res* 2018;**24**(5):1073–81.
15. He L, Huang Y, Ma Z, *et al.* Effects of contrast-enhancement, reconstruction slice thickness and convolution kernel on the diagnostic performance of radiomics signature in solitary pulmonary nodule. *Sci Rep* 2016;**6**:34921.
16. Zhao B, Tan Y, Tsai WY, *et al.* Reproducibility of radiomics for deciphering tumor phenotype with imaging. *Sci Rep* 2016;**6**:23428.
17. Jenkinson M, Beckmann CF, Behrens TE, *et al. FSL Neuroimage* 2012;**62**(2):782–90.
18. Menze BH, Jakab A, Bauer S, *et al.* The multimodal brain tumor Image segmentation benchmark (BRATS). *IEEE Trans Med Imag* 2015;**34**(10):1993–2024.
19. Van Griethuysen JJ, Fedorov A, Parmar C, *et al.* Computational radiomics system to decode the radiographic phenotype. *Canc Res* 2017;**77**(21):e104–7.
20. Zwanenburg A, Leger S, Vallières M, *et al. Image biomarker standardisation initiative*. *arXiv*; 2016. p. 161207003.
21. Gui J, Li H. Penalized Cox regression analysis in the high-dimensional and low-sample size settings, with applications to microarray gene

expression data. *Bioinformatics* 2005;**21**(13):3001–8.
22. Robert T, Jacob B, Jerome F, *et al*. Strong rules for discarding predictors in lasso-type problems. *J Roy Stat Soc B (Stat Methodol))* 2012;**74**(2):245–66.
23. Huang Y, Liu Z, He L, *et al*. Radiomics signature: a potential biomarker for the prediction of disease-free survival in early-stage (I or II) non-small cell lung cancer. *Radiology* 2016;**281**(3):947–57.
24. Nott DJ, Kohn R. Concordance probability and discriminatory power in proportional hazards regression. *Biometrika* 2005;**92**(4):965–70.
25. Goutte C, Gaussier E. A probabilistic interpretation of precision, recall and F-score, with implication for evaluation. In: *Santiago de Compostela, Spain, 21–23 march Advances in information retrieval, 27th European Conference on IR research, ECIR 2005*. Springer; 2005. p. 345–59.
26. Avanzo M, Stancanello J, El Naqa I. Beyond imaging: the promise of radiomics. *Phys Med* 2017;**38**:122–39.
27. Parmar C, Rios Velazquez E, Leijenaar R, *et al*. Robust radiomics feature quantification using semiautomatic volumetric Segmentation. *PLOS ONE* 2014;**9**(7):e102107.
28. Militello C, Rundo L, Vitabile S, *et al*. Gamma Knife treatment planning: MRI brain tumor segmentation and volume measurement based on unsupervised Fuzzy C-Means clustering. *Int J Imag Syst Technol* 2015;**25**(3):213–25.
29. Pereira S, Pinto A, Alves V, *et al*. Brain tumor segmentation using convolutional neural networks in MR Images. *IEEE Trans Med Imag* 2016;**35**(5):1240–51.
30. Ingrisch M, Schneider MJ, Norenberg D, *et al*. Radiomic analysis reveals prognostic information in T1-weighted baseline magnetic resonance imaging in patients with glioblastoma. *Invest Radiol* 2017;**52**(6):360–6.
31. Qi S, Yu L, Li H, *et al*. Isocitrate dehydrogenase mutation is associated with tumor location and magnetic resonance imaging characteristics in astrocytic neoplasms. *Oncol Lett* 2014;**7**(6):1895–902.
32. Abrol S, Kotrotsou A, Salem A, *et al*. Radiomic phenotyping in brain cancer to unravel hidden information in medical images. *Top Magn Reson Imag* 2017;**26**(1):43–53.
33. Chen X, Wei X, Zhang Z, *et al*. Differentiation of true-progression from pseudoprogression in glioblastoma treated with radiation therapy and concomitant temozolomide by GLCM texture analysis of conventional MRI. *Clin Imag* 2015;**39**(5):775–80.
34. Coroller TP, Grossmann P, Hou Y, *et al*. CT-based radiomic signature predicts distant metastasis in lung adenocarcinoma. *Radiother Oncol* 2015;**114**(3):345–50.
35. Ekert K, Hinterleitner C, Horger M. Prognosis assessment in metastatic gastrointestinal stromal tumors treated with tyrosine kinase inhibitors based on CT-texture analysis. *Eur Radiol* 2019;**116**:98–105.
36. Shi W, Zhou L, Peng X, *et al*. HIV-infected patients with opportunistic pulmonary infections misdiagnosed as lung cancers: the clinicoradiologic features and initial application of CT radiomics. *J Thorac Dis* 2019;**11**(6):2274–86.
37. Carrillo JA, Lai A, Nghiemphu PL, *et al*. Relationship between tumor enhancement, edema, IDH1 mutational status, MGMT promoter methylation, and survival in glioblastoma. *AJNR Am J Neuroradiol* 2012;**33**(7):1349–55.
38. Kidd EA, El Naqa I, Siegel BA, *et al*. FDG-PET-based prognostic nomograms for locally advanced cervical cancer. *Gynecol Oncol* 2012;**127**(1):136–40.
39. Huang YQ, Liang CH, He L, *et al*. Development and validation of a radiomics nomogram for preoperative prediction of lymph node metastasis in colorectal cancer. *J Clin Oncol* 2016;**34**(18):2157–64.
40. Lao J, Chen Y, Li ZC, *et al*. A deep learning-based radiomics model for prediction of survival in glioblastoma multiforme. *Sci Rep* 2017;**7**(1):10353.
41. Zhang B, Tian J, Dong D, *et al*. Radiomics features of multiparametric MRI as novel prognostic factors in advanced nasopharyngeal carcinoma. *Clin Canc Res* 2017;**23**(15):4259–69.
42. Ross PL, Gerigk C, Gonen M, *et al*. Comparisons of nomograms and urologists" predictions in prostate cancer. *Semin Urol Oncol* 2002;**20**(2):82–8.
43. Nobusawa S, Watanabe T, Kleihues P, *et al*. IDH1 mutations as molecular signature and predictive factor of secondary glioblastomas. *Clin Canc Res* 2009;**15**(19):6002–7.
44. Metellus P, Coulibaly B, Colin C, *et al*. Absence of IDH mutation identifies a novel radiologic and molecular subtype of WHO grade II gliomas with dismal prognosis. *Acta Neuropathol* 2010;**120**(6):719–29.

Please cite this article as: Su X et al., A radiomics–clinical nomogram for preoperative prediction of IDH1 mutation in primary glioblastoma multiforme, Clinical Radiology, https://doi.org/10.1016/j.crad.2020.07.036